

Copyright WILEY-VCH Verlag GmbH & Co. KGaA, 69469 Weinheim, Germany, 2019.



Supporting Information

for *Adv. Mater. Interfaces*, DOI: 10.1002/admi.201901239

Mn₃O₄ Nanomaterials Functionalized with Fe₂O₃ and ZnO: Fabrication, Characterization, and Ammonia Sensing Properties

Lorenzo Bigiani, Dario Zappa, Chiara Maccato, Alberto Gasparotto, Cinzia Sada, Elisabetta Comini, and Davide Barreca**

Copyright WILEY-VCH Verlag GmbH & Co. KGaA, 69469 Weinheim, Germany, 2019.

Supporting Information

Mn₃O₄ nanomaterials functionalized with Fe₂O₃ and ZnO: fabrication, characterization and ammonia sensing properties

Lorenzo Bigiani, Dario Zappa, Chiara Maccato, Alberto Gasparotto, Cinzia Sada,
Elisabetta Comini, and Davide Barreca**

[*] Dr. L. Bigiani, Prof. C. Maccato, Prof. A. Gasparotto
Department of Chemical Sciences, Padova University and INSTM, 35131 Padova, Italy
E-mail: chiara.maccato@unipd.it

Dr. D. Zappa, Prof. E. Comini
Sensor Lab, Department of Information Engineering, Brescia University, 25133 Brescia, Italy

Prof. C. Sada
Department of Physics and Astronomy, Padova University and INSTM, 35131 Padova, Italy

[*] Dr. D. Barreca
CNR-ICMATE and INSTM, Department of Chemical Sciences, Padova University, 35131
Padova, Italy
E-mail: davide.barreca@unipd.it

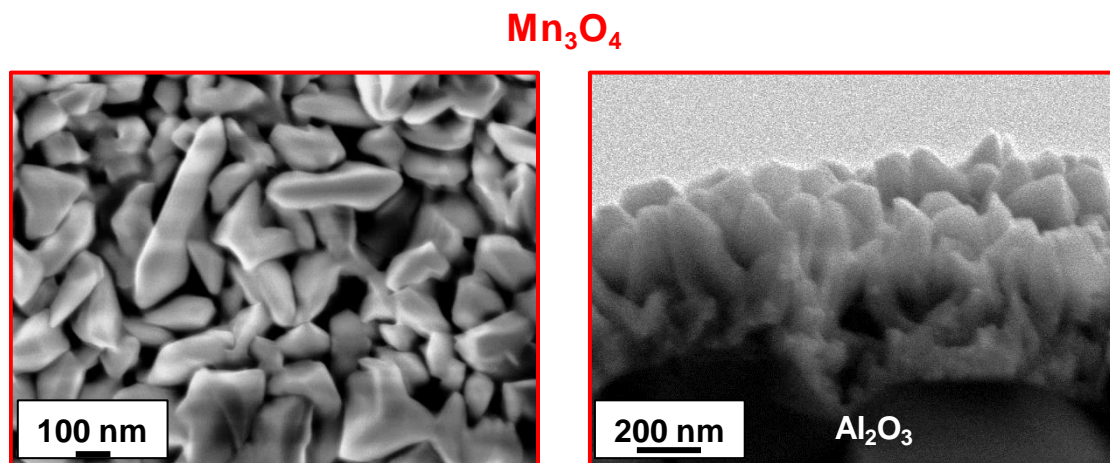
S-1. Characterization**S-1.1. Field emission-scanning electron microscopy (FE-SEM) and energy dispersive X-ray spectroscopy (EDXS)**

Figure S1. Plane-view and cross-sectional field emission-scanning electron microscopy (FE-SEM) micrographs of a bare Mn₃O₄ sample.

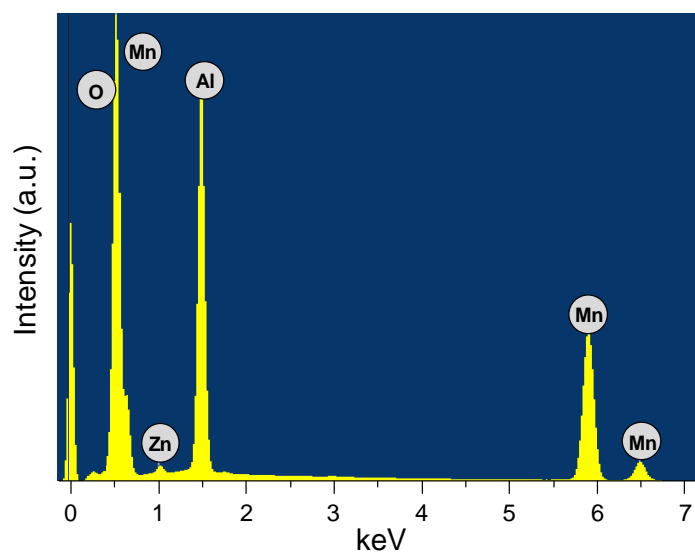


Figure S2. EDXS spectrum for a Mn₃O₄/ZnO specimen.

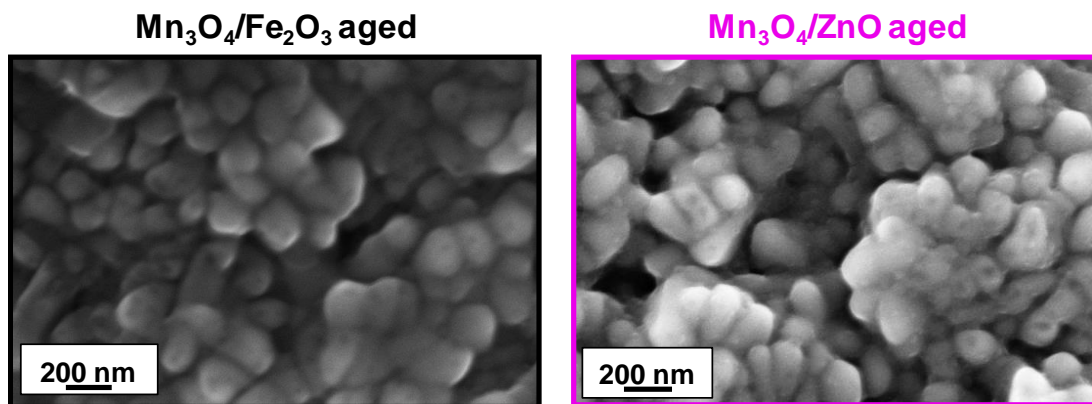


Figure S3. Plane-view FE-SEM micrographs for Mn₃O₄/Fe₂O₃ and Mn₃O₄/ZnO samples after cycled gas sensing tests for one year (average dimensions = (180±40) nm and (170±40) nm for Mn₃O₄/Fe₂O₃ and Mn₃O₄/ZnO, respectively).

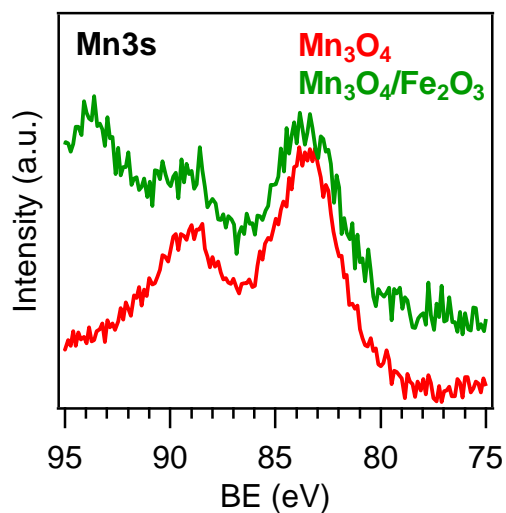
S-1.2. X-ray photoelectron spectroscopy (XPS)

Figure S4. Surface Mn3s photoelectron peaks for Mn₃O₄ and Mn₃O₄/Fe₂O₃ samples. In the case of Mn₃O₄/ZnO specimen, the signal is not reported since it is superimposed with the Zn3p one (<http://srdata.nist.gov/xps>).

S-1-3. Gas sensing tests and data analysis

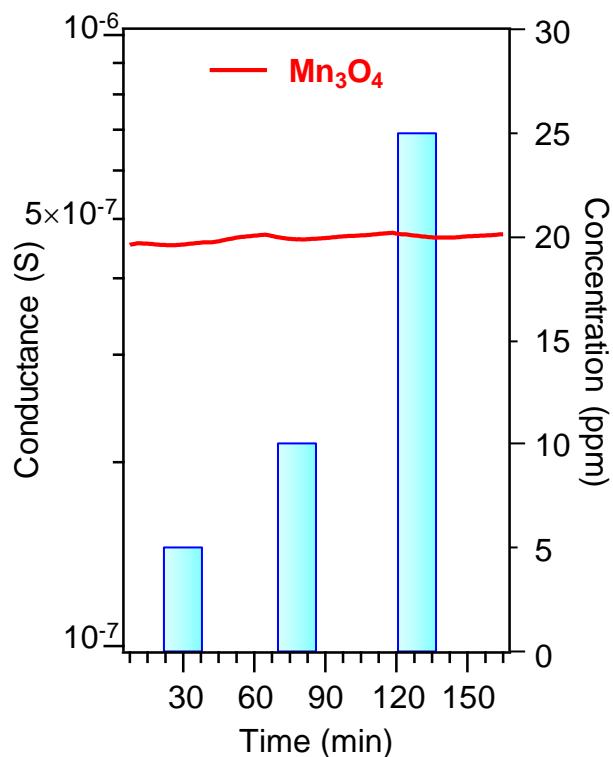


Figure S5. Dynamic response for a Mn_3O_4 specimen upon exposure to ammonia concentration pulses. Working temperature = 300 °C.

sample	<i>K</i>	<i>B</i>
$\text{Mn}_3\text{O}_4/\text{Fe}_2\text{O}_3$	4.9	0.83
$\text{Mn}_3\text{O}_4/\text{ZnO}$	5.4	0.83

Table S1. Parameters obtained by best fitting of the calibration curves (Response = $K \times C^B$) at a working temperature of 300 °C.

The width of the hole accumulation layer (HAL) in pure *p*-type Mn₃O₄ can be estimated by the following relation:^[1]

$$W_{\text{Mn}_3\text{O}_4} = \left[\frac{2\varepsilon_{\text{Mn}_3\text{O}_4} V_0}{q N_{\text{Mn}_3\text{O}_4}} \right]^{1/2}$$

(S1)

where $\varepsilon_{\text{Mn}_3\text{O}_4}$ is the Mn₃O₄ permittivity ($7.94 \times \varepsilon_0$, where ε_0 is the vacuum dielectric permittivity = $8.854 \times 10^{-12} \text{ C}^2 \times \text{N}^{-1} \times \text{m}^{-2}$),^[2] V_0 is the height of the potential barrier established by oxygen adsorption (1.1 eV),^[3] q is the electron charge ($1.602 \times 10^{-19} \text{ C}$), and $N_{\text{Mn}_3\text{O}_4}$ is the hole density in Mn₃O₄ ($2.25 \times 10^{24} \text{ m}^{-3}$).^[4] The calculated $W_{\text{Mn}_3\text{O}_4}$ value is 20.6 nm.

When M_xO_y = Fe₂O₃ or ZnO are loaded onto Mn₃O₄, the HAL thickness is tuned due to the formation of *p–n* Mn₃O₄/M_xO_y junctions, according to the equation:^[1]

$$W'_{\text{Mn}_3\text{O}_4} = \left[\frac{2\varepsilon_{\text{Mn}_3\text{O}_4} \varepsilon_{\text{MxOy}} V_C N_{\text{MxOy}}}{q N_{\text{Mn}_3\text{O}_4} (\varepsilon_{\text{Mn}_3\text{O}_4} N_{\text{Mn}_3\text{O}_4} + \varepsilon_{\text{MxOy}} N_{\text{MxOy}})} \right]^{1/2}$$

(S2)

where $\varepsilon_{\text{MxOy}}$ and N_{MxOy} denote M_xO_y permittivity and majority carrier concentration, respectively ($\varepsilon_{\text{Fe}_2\text{O}_3} = 12.0 \times \varepsilon_0$,^[5] $N_{\text{Fe}_2\text{O}_3} = 5.62 \times 10^{25} \text{ m}^{-3}$;^[6] $\varepsilon_{\text{ZnO}} = 9.67 \times \varepsilon_0$,^[7] $N_{\text{ZnO}} = 6.50 \times 10^{25} \text{ m}^{-3}$),^[8] and V_C is the contact potential variation between M_xO_y and Mn₃O₄, calculated as the difference between the corresponding work function values ($\Phi_{\text{Mn}_3\text{O}_4} = 4.4 \text{ eV}$,^[9] $\Phi_{\text{Fe}_2\text{O}_3} = 5.4 \text{ eV}$,^[10] $\Phi_{\text{ZnO}} = 5.3 \text{ eV}$ ^[8]).

The calculation yields $W'_{\text{Mn}_3\text{O}_4} = 19.5 \text{ nm}$ and 18.5 nm for Mn₃O₄/Fe₂O₃ and Mn₃O₄/ZnO junctions, respectively.

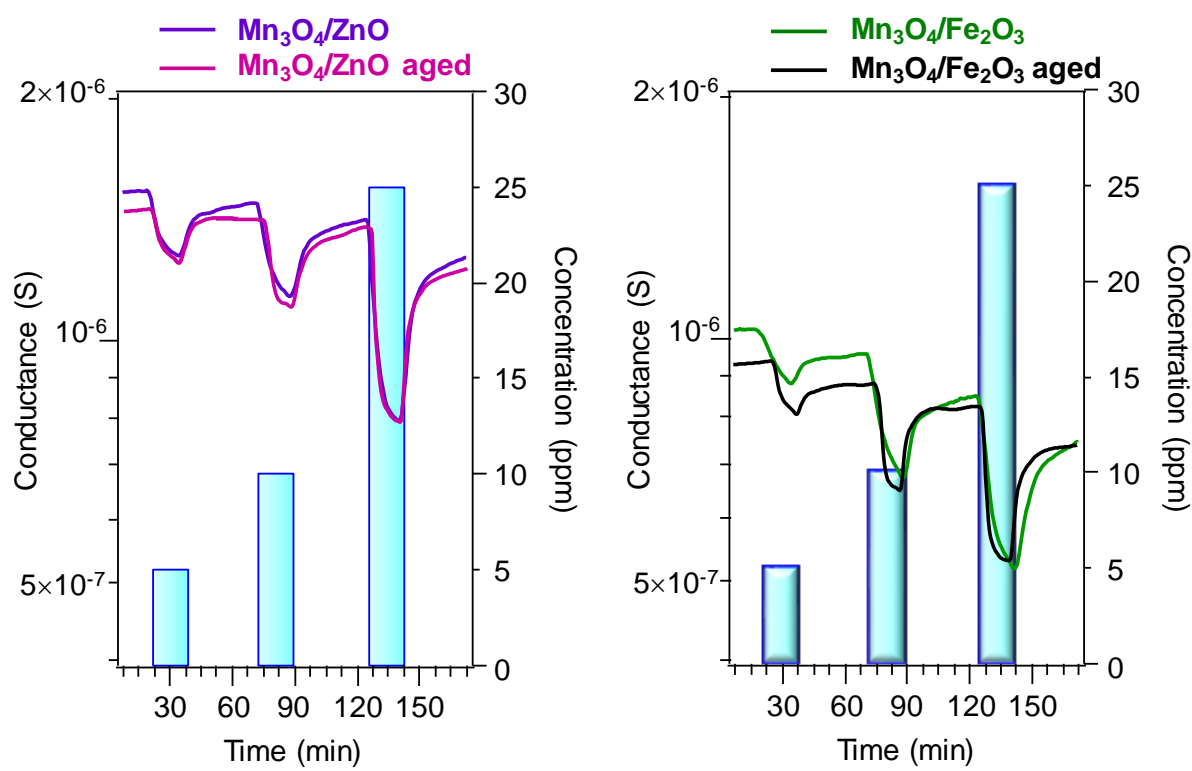


Figure S6. Dynamic responses of $\text{Mn}_3\text{O}_4/\text{ZnO}$ and $\text{Mn}_3\text{O}_4/\text{Fe}_2\text{O}_3$ sensors to NH_3 concentration pulses after one year of cycled tests. Working temperature = 300 °C.

References

- [1] S.-W. Choi, A. Katoch, J.-H. Kim, S. S. Kim, *ACS Appl. Mater. Interf.* **2015**, *7*, 647.
- [2] L. Ben Said, R. Boughalmi, A. Inoubli, M. Amlouk, *Appl. Microsc.* **2017**, *47*, 131.
- [3] T. Larbi, B. Ouni, A. Boukhachem, K. Boubaker, M. Amlouk, *Mater. Res. Bull.* **2014**, *60*, 457.
- [4] T. Larbi, M. Haj Lakhdar, A. Amara, B. Ouni, A. Boukhachem, A. Mater, M. Amlouk, *J. Alloys Compd.* **2015**, *626*, 93.
- [5] D. R. Lide, H. P. R. Frederikse, *Handbook of Chemistry and Physics*, 75th Ed., CRC Press, Inc.: Boca Raton,, 1995, pp. 12-53.
- [6] H. K. Mulmudi, N. Mathews, X. C. Dou, L. F. Xi, S. S. Pramana, Y. M. Lam, S. G. Mhaisalkar, *Electrochem. Commun.* **2011**, *13*, 951.
- [7] F. S. Mahmood, R. D. Gould, A. K. Hassan, H. M. Salih, *Thin Solid Films* **1995**, *270*, 376.
- [8] T. Minami, T. Miyata, T. Yamamoto, *Surf. Coat. Technol.* **1998**, *108-109*, 583.
- [9] G. Maniak, P. Stelmachowski, F. Zasada, W. Piskorz, A. Kotarba, Z. Sojka, *Catalysis Today* **2011**, *176*, 369.
- [10] Z. Fan, X. Wen, S. Yang, J. G. Lu, *Appl. Phys. Lett.* **2005**, *87*, 013113.